Analytic Estimation Method of Forced Oscillation Amplitude Under Stochastic Continuous Disturbances

Hongyu Li, *Student Member, IEEE*, Ping Ju, *Senior Member, IEEE*, Chun Gan, *Member, IEEE*, Yufei Tang, *Member, IEEE*, Yiping Yu, *Member, IEEE*, and Yilu Liu, *Fellow, IEEE*

***Abstract*—This paper proposes an analytic method for the amplitude estimation of the forced oscillation under stochastic continuous disturbances (SCDs). There is considerable interest in the integration of intermittent renewable energy resources into a power system, which leads to the power system in an environment with SCDs. Thus, the forced oscillation issues under SCDs are of concern. In this paper, the SCDs are described as continuous-time stochastic processes, and then the systems under SCDs are modeled by stochastic differential algebraic equations. Furthermore, by employing stochastic theory, an efficient analytic method for calculating the statistics of system states during the forced oscillation is proposed. Moreover, a novel forced oscillation phenomenon, which presents system states oscillate with stationary distributions under SCDs, is clearly characterized and theoretically explained. Based on the proposed analytic method, a scheme is put forth to estimate amplitudes of system states during forced oscillation under SCDs. Finally, compared to Monte Carlo simulation, the proposed scheme has two significant advantages. First, the proposed scheme offers a fast and effective solution for engineering applications. Second, the impact mechanism of SCDs on forced oscillation in power system is clearer, by the proposed scheme.**

***Index Terms*—Stochastic differential algebraic equation, linearized stochastic differential equations, stochastic process, amplitude estimation, Monte Carlo simulation.**

Manuscript received August 17, 2017; revised December 29, 2017 and April 17, 2018; accepted June 9, 2018. Date of publication June 19, 2018; date of current version June 19, 2019. This work was support in part by the 111 Project of Renewable Energy and Smart Grid under Grant B14022, in part by the National Basic Research Program of China under Grant 2013CB228204, and in part by the National Natural Science Foundation of China under Grant 51422701 and Grant 51707056. Paper no. TSG-01201-2017. *(Corresponding author: Ping Ju.)*

H. Li is with the College of Energy and Electrical Engineering, Hohai University, Nanjing 211100, China, and also with the Department of Electrical Engineering and Computer Science, University of Tennessee, Knoxville, TN 37996 USA (e-mail: hongyu.li.1990@gmail.com).

P. Ju and Y. Yu are with the College of Energy and Electrical Engineering, Hohai University, Nanjing 211100, China (e-mail: pju@hhu.edu.cn; yyiping@hhu.edu.cn).

C. Gan and Y. Liu are with the Department of Electrical Engineering and Computer Science, University of Tennessee, Knoxville, TN 37996 USA (e-mail: cgan@utk.edu; liu@utk.edu).

Y. Tang is with the Department of Computer and Electrical Engineering and Computer Science, Institute for Sensing and Embedded Network Systems Engineering, Florida Atlantic University, Boca Raton, FL 33431 USA (e-mail: tangy@fau.edu).

Color versions of one or more of the figures in this paper are available online at http://ieeexplore.ieee.org.

Digital Object Identifier 10.1109/TSG.2018.2848637

I. Introduction

With the integration of intermittent renewable energy in power systems, their random nature has attracted much attention [1]–[4]. One of the major concerns is whether their random nature could impact small-signal stability [5]–[9]. From the view of small-signal stability, the randomness can be classified into two main categories [10], [11]: (1) randomness of the state matrix coefficients, which are related to the randomness from nodal loads, operating status of generation units, change of generation unit's dispatch, parameters of transmission lines, and parameters of control devices, etc. [12]–[14]; and (2) external stochastic excitation, which is described as the stochastic continuous disturbances (SCDs) [10]. Deterministic analysis approaches are unable to fully reveal the impact of randomness on the power system, so the stochastic method is desired.

Most research has been conducted on small-signal stability under the randomness of state matrix coefficients [15], which is usually called as "probabilistic small-signal stability" (PSSS). PSSS's aim is focused on analyzing the statistics of oscillatory modes and the damping of those oscillatory modes to check whether negative damping oscillation occurs. Matrix operations are primary analysis tools in PSSS. In [15], a nonlinear analytical methodology is proposed for PSSS of power systems with high penetration wind generation. In [16], the coordination of power system stabilizers and static VAR compensator damping controller is presented to improve PSSS of power systems with high penetration wind generation. PSSS of power systems with offshore wind generation is investigated in [17], by using cumulant-based theory. A quasi-Monte Carlo based method is proposed to analyze PSSS of power systems with the plug-in electric vehicle and wind power integration [18]. In [19], the stochastic response surface method is utilized to analyze the PSSS of the power system with uncertainties in correlated photovoltaic and loads. Impacts of the stochastic photovoltaic system generation on small-signal stability are investigated in [20], by employing a PSSS method.

Much attention is attracted to small-signal analysis under external SCDs, though few attempts have been made to this difficult issue. Even if a dynamic system can tolerate one severe fault at its equilibrium point, cumulative effects of SCDs can cause its state trajectories to leave any bounded domain after a sufficiently long time [21]–[23]. SCDs can be

regarded as external perturbation for the system, so small-signal analysis under SCDs belongs to the forced oscillation issues. In [10], a good solution to analyze the small-signal stability under SCDs is presented, while the method's accuracy should be improved. A systematic framework to analyze small-signal power-injections stochastic variations in power systems is proposed in [24], while forced oscillation issues under SCDs are not addressed and the results are mainly given by theoretical statistics.

In a short time frame, the probability density function that is driving the SCDs is usually described as the Gaussian distribution function. In [25], power systems influenced by stochastic perturbations in load and variable renewable generation are modeled by stochastic differential-algebraic equations, where the Gaussian distribution is used. The SCDs from the renewable-based electricity generation are considered as Gaussian-distribution-based stochastic processes in [26], and then the effects of these disturbances on power system dynamics are studied. In [27], a stochastic model which includes uncertainties in the system load at the wind generator bus is presented, in which the Gaussian distribution is used to describe their distribution. Furthermore, power systems under SCDs can be modeled as stochastic differential algebraic equations (SDAEs) [28]–[30]. A systematic method to model power systems under stochastic perturbations is presented in [31], by using SDAEs. In [32], a stochastic model based on SDAEs is employed to describe power systems with variable wind power. By utilizing SDAEs, continuous wind speed models are proposed in [33]. Hence, this paper implements the most commonly used SDAEs to analyze the forced oscillation in the power system under SCDs.

In recent decades, small-signal stability analysis of power systems under randomness has been deeply considered, but there are still some issues needing solution: (1) the majority of existing analytic methods focus on randomness in the state matrix coefficients, and few papers research small-signal stability under external SCDs [14]–[20]; (2) for the small-signal stability under SCDs, analytic methods which can offer sufficient accuracy with high efficiency still not appear; (3) analysis results are usually given by statistics, while results which meet engineer's needs are not proposed, such as the oscillation amplitude of system states.

To deal with the issues mentioned above, this paper proposes an efficient analytic estimation method for forced oscillation amplitude in power systems under SCDs. SCDs are described as continuous-time stochastic processes, and then power systems under SCDs are modeled by SDAEs. Furthermore, an amplitude estimation scheme is presented to investigate the forced oscillation under SCDs. Compared to Monte Carlo simulation, the proposed scheme shows two significant advantages: first, the higher efficiency with similar accuracy; second, clearer impact mechanism of SCDs on the forced oscillation.

This paper is organized as follows: Section II introduces analysis issues faced with forced oscillation in the power system under SCDs. Section III presents the models of multi-machine power systems under SCDs. Section IV proposes the analytic estimation method for forced oscillation amplitude under SCDs. Section V gives simulation cases. Section VI offers conclusions. An example of the power system under SCDs is shown in Appendix.

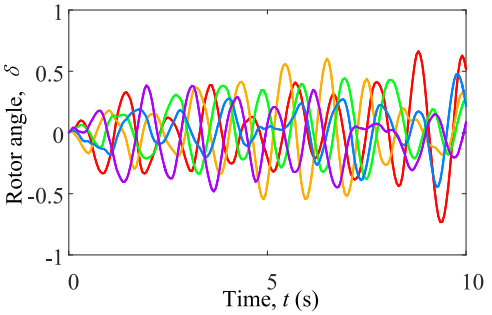

Fig. 1. Rotor angle oscillation trajectories of an SMIB system under SCDs.

II. Forced Oscillation in Power System Under SCDs

It is known that forced oscillation is usually excited by deterministic continuous disturbances, whose frequencies are close or equal to system natural frequencies [34]. In the conventional deterministic analysis approaches of forced oscillation, disturbances are assumed with deterministic characteristics in the frequency domain, and thus the system states oscillate along with deterministic characteristics in the frequency domain [34]. With the increasing randomness in power system, these deterministic methods will face new problems, due to no consideration of the random nature. For example, intermittent renewable energy is introducing SCDs into the power system, whose frequencies and amplitudes are stochastic. To show the forced oscillation under SCDs, Fig. 1 gives five rotor angle trajectories of a single-machine infinite-bus system (SMIB) under SCDs. In this SMIB system, all real parts of system eigenvalues are negative, and the initial simulation value is set as the stable equilibrium point. It can be seen that the rotor angle oscillates with stochastic amplitudes over time, which cannot be revealed and explained by the conventional deterministic analysis approaches. In other words, for the forced oscillation under SCDs, conventional deterministic methods without consideration of the random nature are incomplete. Thus, stochastic analytic methods which can offer a more comprehensive analysis are desired.

III. Stochastic Model of the System Under SCDs

A. SCDs in Power Systems

With the increasing penetration of intermittent renewable energy, SCDs become more and more considerable. In this paper, for modeling SCDs, an approach similar to [10] and [25]–[32] is adopted. Specifically, SCDs are modeled as continuous-time stochastic processes, additive to the power system models. For example, when the SCDs are considered from the renewable generation, the mechanical power input of a wind turbine can be expressed as [10] and [35]:

$$P_m = P_{m,0} + \Delta P_m \tag{1}$$

where P_m denotes the mechanical power including SCDs; $P_{m,0}$ denotes the low-frequency mechanical power, which is

assumed to be constant and equal to the mean value of P_m [35]; and ΔP_m denotes the high-frequency SCDs, which can be described by an additive continuous-time stochastic process.

B. Nonlinear Stochastic Model of a Power System Under SCDs

The deterministic model of a power system is usually described through a set of differential algebraic equations (DAEs) as follows [31]:

$$\begin{cases} d\boldsymbol{X}(t) = \boldsymbol{f}[\boldsymbol{X}(t), \boldsymbol{Y}(t)]dt \\ \boldsymbol{O} = \boldsymbol{g}[\boldsymbol{X}(t), \boldsymbol{Y}(t)] \end{cases} \tag{2}$$

where $\boldsymbol{X}(t)$ denotes the vector of state variables; $\boldsymbol{Y}(t)$ denotes the vector of algebraic variables; $\boldsymbol{f}$ denotes the vector of nonlinear functions in differential equations; $\boldsymbol{g}$ denotes the vector of nonlinear functions in algebraic equations; and $\boldsymbol{O}$ denotes a null matrix.

After considering the SCDs, continuous-time stochastic processes are introduced into the DAEs (2). Then, a set of SDAEs, which can be used to describe power systems under SCDs, is built as follows [10], [25]–[32]:

$$\begin{cases} d\boldsymbol{X}(t) = \boldsymbol{f}[\boldsymbol{X}(t), \boldsymbol{Y}(t)]dt + \boldsymbol{K}d\boldsymbol{B}(t) \\ \boldsymbol{O} = \boldsymbol{g}[\boldsymbol{X}(t), \boldsymbol{Y}(t)] \end{cases} \tag{3}$$

where $\boldsymbol{K}\mathrm{d}\boldsymbol{B}(t)$ denotes the vector of SCDs; $\boldsymbol{B}(t)$ denotes a vector whose elements are independent standard Wiener processes; and $\boldsymbol{K}$ denotes the covariance matrix of SCDs, which means the intensity and correlation of SCDs.

C. Linearized Stochastic Model of a Power System Under SCDs

Based on the equilibrium point (i.e., the steady state) of the nonlinear model (2), one can linearize (3) around it [24]. The linearized stochastic model of a power system under SCDs can be expressed as follows:

$$\begin{bmatrix} d\Delta\boldsymbol{X}(t) \\ \boldsymbol{O} \end{bmatrix} = \begin{bmatrix} \boldsymbol{f}_{\boldsymbol{X}} & \boldsymbol{f}_{\boldsymbol{Y}} \\ \boldsymbol{g}_{\boldsymbol{X}} & \boldsymbol{g}_{\boldsymbol{Y}} \end{bmatrix} \begin{bmatrix} \Delta\boldsymbol{X}(t) \\ \Delta\boldsymbol{Y}(t) \end{bmatrix} dt + \begin{bmatrix} \boldsymbol{K}d\boldsymbol{B}(t) \\ \boldsymbol{O} \end{bmatrix} \tag{4}$$

where $\Delta\boldsymbol{X}(t) = \boldsymbol{X}(t) - \boldsymbol{X}(0)$ and $\Delta\boldsymbol{Y}(t) = \boldsymbol{Y}(t) - \boldsymbol{Y}(0)$; $\boldsymbol{X}(0)$ and $\boldsymbol{Y}(0)$ denote the initial point, which is assumed as the equilibrium point of the system in this paper; $\boldsymbol{f}_{\boldsymbol{X}}$ and $\boldsymbol{f}_{\boldsymbol{Y}}$ are the Jacobian matrixes of $\boldsymbol{f}$ with respect to $\boldsymbol{X}$ and $\boldsymbol{Y}$, which can be obtained by differential derivatives. $\boldsymbol{g}_{\boldsymbol{X}}$ and $\boldsymbol{g}_{\boldsymbol{Y}}$ are the Jacobian matrixes of $\boldsymbol{g}$ with respect to $\boldsymbol{X}$ and $\boldsymbol{Y}$, which can be can be taken straight from the power flow Jacobian matrix.

Eliminating the algebraic equation in (4), one can obtain the linearized stochastic model as a set of linearized stochastic differential equations (LSDEs), which is as follows:

$$d\Delta\boldsymbol{X}(t) = \boldsymbol{A}\Delta\boldsymbol{X}(t)dt + \boldsymbol{K}d\boldsymbol{B}(t) \tag{5}$$

where $\boldsymbol{A}$ denotes the state matrix of the linearized system and equals to $\boldsymbol{f}_{\boldsymbol{X}} - \boldsymbol{f}_{\boldsymbol{Y}}(\boldsymbol{g}_{\boldsymbol{Y}})^{-1}\boldsymbol{g}_{\boldsymbol{X}}$ [25].

Many stochastic power system models have been already proposed in the existing papers [10], [21]–[32], so the power system models used in this paper are given in generic terms. To show the stochastic model and its linearization, a specific power system model under SCDs is given as an example in Appendix, which is similar to the models in [30], [36], and [37].

IV. Stochastic Analysis of Forced Oscillation Under SCDs

In this section, the stochastic analysis for forced oscillation is carried out based on the linearized stochastic model (5). This section is the core of this paper, which is carefully organized as follows: firstly, the explicit formulation of solution for LSDEs (5) is presented; secondly, the mean and covariance of system states over time, which are closely related to the characteristics of forced oscillation, are analytically solved; thirdly, a novel oscillation phenomenon, which presents that the system states oscillate with stationary distributions, is clearly characterized and theoretically explained; fourthly, an amplitude estimation method is put forward to estimate the amplitudes of system states during the forced oscillation under SCDs.

A. Explicit Formulation of the Solution to LSDEs

Before giving the explicit formulation of the solution to LSDEs (5), an exponential function of a general n^{th}-order square matrix $\boldsymbol{M}$ is firstly defined as follows:

$$\exp(\boldsymbol{M}) = \sum_{n=0}^{+\infty} (\boldsymbol{M}^n / n!) \tag{6}$$

where $n!$ denotes the factorial of a non-negative integer n.

In the following, the explicit formulation of the solution to LSDEs (5) will be deduced. Multiplying both sides of LSDEs (5) by exp(-$\boldsymbol{A}t$), one obtains

$$\begin{aligned} \exp(-\boldsymbol{A}t)d\Delta\boldsymbol{X}(t) = {} & \exp(-\boldsymbol{A}t)\boldsymbol{A}\Delta\boldsymbol{X}(t)dt \\ & + \exp(-\boldsymbol{A}t)\boldsymbol{K}d\boldsymbol{B}(t). \end{aligned} \tag{7}$$

By the matrix calculus [38], (7) can be expressed as

$$d\big[\exp(-\boldsymbol{A}t)\Delta\boldsymbol{X}(t)\big] = \exp(-\boldsymbol{A}t)\boldsymbol{K}d\boldsymbol{B}(t). \tag{8}$$

Let s denote t in (8), and then the integral of (8) over the time interval $[t_0, t]$ is deduced as follows:

$$\exp(-\boldsymbol{A}t)\Delta\boldsymbol{X}(t) - \exp(-\boldsymbol{A}t_0)\Delta\boldsymbol{X}(t_0) = \int_{t_0}^{t} \exp(-\boldsymbol{A}s)\boldsymbol{K}d\boldsymbol{B}(s). \tag{9}$$

Multiplying both sides of (9) by exp($\boldsymbol{A}t$), one obtains

$$\Delta\boldsymbol{X}(t) = \exp[\boldsymbol{A}(t-t_0)]\Delta\boldsymbol{X}(t_0) + \int_{t_0}^{t} \exp[\boldsymbol{A}(t-s)]\boldsymbol{K}d\boldsymbol{B}(s). \tag{10}$$

Equation (10) is the explicit formulation of the solution to LSDEs (5). It was proven that $\int_{t_0}^{t} \exp[\boldsymbol{A}(t-s)]\boldsymbol{K}d\boldsymbol{B}(s)$ follows Gaussian distributions in [39], and thus system states $\Delta\boldsymbol{X}(t)$ follow Gaussian distributions. For the Gaussian distribution, the mean and variance are two key factors. In the following section, the mean and variance of system states over time will be analytically solved, which are closely related to the characteristics of forced oscillation under SCDs.

B. Mean of System States During Forced Oscillation Under SCDs

According to the definition of mean, the system states mean during forced oscillation under SCDs are expressed as follows:

$$E[\Delta \boldsymbol{X}(t)] = E\left\{\exp[\boldsymbol{A}(t-t_0)]\Delta \boldsymbol{X}(t_0) + \int_{t_0}^{t} \exp[\boldsymbol{A}(t-s)]\boldsymbol{K}d\boldsymbol{B}(s)\right\} = E\{\exp[\boldsymbol{A}(t-t_0)]\Delta \boldsymbol{X}(t_0)\} + E\left\{\int_{t_0}^{t} \exp[\boldsymbol{A}(t-s)]\boldsymbol{K}d\boldsymbol{B}(s)\right\}. \tag{11}$$

By the definition of Itô integral [39], the following formulation can be deduced from (11)

$$\begin{aligned} E[\Delta \boldsymbol{X}(t)] &= E\{\exp[\boldsymbol{A}(t-t_0)]\Delta \boldsymbol{X}(t_0)\} \\ &\quad + E\left\langle \lim_{\lambda\to 0}\sum_{i=0}^{k-1}\left\{\exp[\boldsymbol{A}(t-t_i)]\boldsymbol{K}\left[\boldsymbol{B}(t_{i+1})-\boldsymbol{B}(t_i)\right]\right\}\right\rangle \\ &= E\{\exp[\boldsymbol{A}(t-t_0)]\Delta \boldsymbol{X}(t_0)\} \\ &\quad + \lim_{\lambda\to 0}\sum_{i=0}^{k-1}\left\{\exp[\boldsymbol{A}(t-t_i)]\boldsymbol{K}E\left[\boldsymbol{B}(t_{i+1})-\boldsymbol{B}(t_i)\right]\right\} \\ &= E\{\exp[\boldsymbol{A}(t-t_0)]\Delta \boldsymbol{X}(t_0)\} \end{aligned} \tag{12}$$

where $t_k = t$; λ is equal to the maximum value of $t_{i+1} - t_i$ $(i = 0, 1, \ldots, k-1)$; $E[\boldsymbol{B}(t_i+1) - \boldsymbol{B}(t_i)] = 0$, because of the characteristic of Wiener process.

In this paper, the parameters $\boldsymbol{A}$ and initial system states $\Delta \boldsymbol{X}(t_0)$ are assumed without randomness. Thus, one obtains

$$E[\Delta \boldsymbol{X}(t)] = \exp[\boldsymbol{A}(t-t_0)]\Delta \boldsymbol{X}(t_0). \tag{13}$$

Equation (13) is the explicit formulation of the solution to LSDEs (5) system states mean.

C. The Variance of System States During Forced Oscillation Under SCDs

The system states variance is an important factor, which indirectly indicates how far system states will leave the equilibrium point during the forced oscillation under SCDs. In this paper, the covariance matrix is investigated, which includes both the variance and covariance of system states. According to the definition of the covariance matrix, the system states covariance matrix can be expressed as follows:

$$Var[\Delta \boldsymbol{X}(t)] = E\left\langle\{\Delta \boldsymbol{X}(t) - E[\Delta \boldsymbol{X}(t)]\}\{\Delta \boldsymbol{X}(t) - E[\Delta \boldsymbol{X}(t)]\}^T\right\rangle. \tag{14}$$

Substituting $\Delta \boldsymbol{X}(t)$ (10) and its mean (13) into the covariance matrix (14), the following formulation can be deduced

$$Var[\Delta \boldsymbol{X}(t)] = E\left\langle\left\{\int_{t_0}^{t} \exp[\boldsymbol{A}(t-s)]\boldsymbol{K}d\boldsymbol{B}(s)\right\} \times \left\{\int_{t_0}^{t} \exp[\boldsymbol{A}(t-s)]\boldsymbol{K}d\boldsymbol{B}(s)\right\}^T\right\rangle. \tag{15}$$

By the definition of Itô integral [39], the following equation can be further deduced from (15)

$$\begin{aligned} &Var[\Delta \boldsymbol{X}(t)] \\ &= E\left\langle\left\{\lim_{\lambda\to 0}\sum_{i=0}^{k-1}\exp[\boldsymbol{A}(t-t_i)]\boldsymbol{K}\left[\boldsymbol{B}(t_{i+1})-\boldsymbol{B}(t_i)\right]\right\} \right. \\ &\qquad \left.\left\{\lim_{\lambda\to 0}\sum_{j=0}^{k-1}\exp\left[\boldsymbol{A}(t-t_j)\right]\boldsymbol{K}\left[\boldsymbol{B}(t_{j+1})-\boldsymbol{B}(t_j)\right]\right\}^T\right\rangle \\ &= E\left\langle\lim_{\lambda\to 0}\sum_{0\le i,j\le k-1}\left\{\exp[\boldsymbol{A}(t-t_i)]\boldsymbol{K}\left[\boldsymbol{B}(t_{i+1})-\boldsymbol{B}(t_i)\right]\right. \right. \\ &\qquad \left.\left.\times\left[\boldsymbol{B}(t_{j+1})-\boldsymbol{B}(t_j)\right]^T\boldsymbol{K}^T\exp\left[\boldsymbol{A}^T(t-t_j)\right]\right\}\right\rangle \\ &= \lim_{\lambda\to 0}\sum_{0\le i,j\le k-1}\left\langle\exp[\boldsymbol{A}(t-t_i)]\boldsymbol{K}E\left\{\left[\boldsymbol{B}(t_{i+1})-\boldsymbol{B}(t_i)\right]\right.\right. \\ &\qquad \left.\left.\times\left[\boldsymbol{B}(t_{j+1})-\boldsymbol{B}(t_j)\right]^T\right\}\boldsymbol{K}^T\exp\left[\boldsymbol{A}^T(t-t_j)\right]\right\rangle \\ &= \lim_{\lambda\to 0}\sum_{\substack{0\le i,\, j\le k-1,\\ \text{and } i=j}}\left\langle\exp[\boldsymbol{A}(t-t_i)]\boldsymbol{K}E\left\{\left[\boldsymbol{B}(t_{i+1})-\boldsymbol{B}(t_i)\right]\right.\right. \\ &\qquad \left.\left.\times\left[\boldsymbol{B}(t_{j+1})-\boldsymbol{B}(t_j)\right]^T\right\}\boldsymbol{K}^T\exp\left[\boldsymbol{A}^T(t-t_j)\right]\right\rangle \\ &+ \lim_{\lambda\to 0}\sum_{\substack{0\le i,j\le k-1,\\ \text{and} i\ne j}}\left\langle\exp[\boldsymbol{A}(t-t_i)]\boldsymbol{K}E\left\{\left[\boldsymbol{B}(t_{i+1})-\boldsymbol{B}(t_i)\right]\right.\right. \\ &\qquad \left.\left.\times\left[\boldsymbol{B}(t_{j+1})-\boldsymbol{B}(t_j)\right]^T\right\}\boldsymbol{K}^T\exp\left[\boldsymbol{A}^T(t-t_j)\right]\right\rangle \end{aligned} \tag{16}$$

where $t_k = t$; λ is equal to the maximum value of $t_{i+1} - t_i$ $(i = 0, 1, \ldots, k-1)$ and $t_{j+1} - t_j$ $(j = 0, 1, \ldots, k-1)$.

By the characteristic of Wiener processes [39], one obtains

$$E\left\{[\boldsymbol{B}(t_{i+1})-\boldsymbol{B}(t_i)][\boldsymbol{B}(t_{j+1})-\boldsymbol{B}(t_j)]^T\right\} = \begin{cases} t_{i+1}-t_i, & \text{if } i=j \\ 0, & \text{if } i\ne j. \end{cases} \tag{17}$$

Substituting (17) into the covariance matrix (16), one obtains

$$\begin{aligned} Var[\Delta \boldsymbol{X}(t)] &= \lim_{\lambda\to 0}\sum_{i=0}^{k-1}\left\{\exp[\boldsymbol{A}(t-t_i)]\boldsymbol{K}\boldsymbol{K}^T\exp\left[\boldsymbol{A}^T(t-t_i)\right](t_{i+1}-t_i)\right\} \\ &= \int_{t_0}^{t}\exp[\boldsymbol{A}(t-s)]\boldsymbol{K}\boldsymbol{K}^T\exp\left[\boldsymbol{A}^T(t-s)\right]ds. \end{aligned} \tag{18}$$

By utilizing (18), one can calculate the system states covariance matrix during the forced oscillation. However, the solution to covariance matrix (18) is not exactly analytic, which lend itself difficult to calculate, due to the existence of the integral. In the following, matrix operations are adopted to eliminate the integral in (18), and then an analytic expression without the integral is deduced.

To analyze the forced oscillation, the analysis system is assumed to be small-signal stable [40], which means all the eigenvalues exist and have negative real parts. By the eigendecomposition [34], system state matrix $\boldsymbol{A}$ can be factorized as

$$\boldsymbol{A} = \boldsymbol{P}\boldsymbol{\Lambda}\boldsymbol{P}^{-1} \tag{19}$$

where $\boldsymbol{\Lambda}$ denotes the eigenvalue matrix, and $\boldsymbol{\Lambda} = \text{diag}[\lambda_1, \lambda_2, \ldots, \lambda_i, \ldots]$; and $\boldsymbol{P}$ denotes the similarity transformation from $\boldsymbol{A}$ to $\boldsymbol{\Lambda}$, whose i^{th} column is the eigenvector.

Substituting (19) into exp[$\boldsymbol{A}$(*t*-*s*)], one obtains

$$\exp[\boldsymbol{A}(t-s)] = \boldsymbol{P}\boldsymbol{\Gamma}\boldsymbol{P}^{-1} \tag{20}$$

where $\boldsymbol{\Gamma} = \text{diag}[\exp(\lambda_1 t - \lambda_1 s), \exp(\lambda_2 t - \lambda_2 s), \ldots, \exp(\lambda_i t - \lambda_i s), \ldots]$.

Incorporating exp[$\boldsymbol{A}$(*t*-*s*)] (20) into $Var[\Delta \boldsymbol{X}(t)]$ in (18), one obtains

$$\begin{aligned} Var[\Delta \boldsymbol{X}(t)] &= \int_{t_0}^{t} \boldsymbol{P}\boldsymbol{\Gamma}\boldsymbol{P}^{-1}\boldsymbol{K}\boldsymbol{K}^T\left(\boldsymbol{P}^{-1}\right)^T\boldsymbol{\Gamma}^T\boldsymbol{P}^T ds \\ &= \boldsymbol{P}\left[\int_{t_0}^{t} \boldsymbol{\Gamma}\boldsymbol{P}^{-1}\boldsymbol{K}\boldsymbol{K}^T\left(\boldsymbol{P}^{-1}\right)^T\boldsymbol{\Gamma}^T ds\right]\boldsymbol{P}^T. \end{aligned} \tag{21}$$

Let $\boldsymbol{F}$ and $\boldsymbol{G}$ denote the matrix $\boldsymbol{P}^{-1}\boldsymbol{K}\boldsymbol{K}^T(\boldsymbol{P}^{-1})^T$ and $\boldsymbol{\Gamma}\boldsymbol{P}^{-1}\boldsymbol{K}\boldsymbol{K}^T(\boldsymbol{P}^{-1})^T\boldsymbol{\Gamma}^T$, respectively. Considering that $\boldsymbol{\Gamma}$ is a diagonal matrix, one deduces

$$\begin{aligned} \boldsymbol{G}(i,j) &= \boldsymbol{F}(i,j)\exp(\lambda_i t - \lambda_i s)\exp\left(\lambda_j t - \lambda_j s\right) \\ &= \boldsymbol{F}(i,j)\exp\left[\left(\lambda_i + \lambda_j\right)(t-s)\right] \end{aligned} \tag{22}$$

where $\boldsymbol{F}(i, j)$ and $\boldsymbol{G}(i, j)$ denote the $(i,j)^{\text{th}}$ element of $\boldsymbol{F}$ and $\boldsymbol{G}$ in the i^{th} row and j^{th} column, respectively.

Let $\boldsymbol{H}$ denote the matrix $\int_{t_0}^{t} \boldsymbol{\Gamma}\boldsymbol{P}^{-1}\boldsymbol{K}\boldsymbol{K}^T(\boldsymbol{P}^{-1})^T\boldsymbol{\Gamma}^T ds$. Furthermore, the integral of the element of $\boldsymbol{G}$ (22) can be obtained as

$$\begin{aligned} \boldsymbol{H}(i,j) &= \int_{t_0}^{t} \boldsymbol{G}(i,j)ds = \int_{t_0}^{t} \boldsymbol{F}(i,j)\exp\left[\left(\lambda_i + \lambda_j\right)(t-s)\right]ds \\ &= \boldsymbol{F}(i,j)\left\{\exp\left[\left(\lambda_i + \lambda_j\right)(t-t_0)\right] - 1\right\}/\left(\lambda_i + \lambda_j\right) \end{aligned} \tag{23}$$

where $\boldsymbol{H}(i, j)$ denotes the $(i,j)^{\text{th}}$ element of $\boldsymbol{H}$.

Based on (23), $\boldsymbol{H}$ can be expressed as

$$\boldsymbol{H} = \boldsymbol{F} \circ \boldsymbol{J} \tag{24}$$

where "$\circ$" denotes Hadamard product [41]; and $\boldsymbol{J}$ denotes a matrix whose $(i,j)^{\text{th}}$ element is $\{\exp[(\lambda_i + \lambda_j)(t\text{-}t_0)]\text{-}1\}/(\lambda_i + \lambda_j)$.

Substituting $\boldsymbol{H}$ (24) into $Var[\Delta \boldsymbol{X}(t)]$ (21), one obtains

$$Var[\Delta \boldsymbol{X}(t)] = \boldsymbol{P}[\boldsymbol{F} \circ \boldsymbol{J}]\boldsymbol{P}^T = \boldsymbol{P}\left\{\left[\boldsymbol{P}^{-1}\boldsymbol{K}\boldsymbol{K}^T\left(\boldsymbol{P}^{-1}\right)^T \circ \boldsymbol{J}\right]\right\}P^T. \tag{25}$$

Equation (25) is the explicit formulation of the solution to LSDEs (5) system states covariance matrix, where there is no integral.

The above derivation (in Sections IV-B and IV-C) is complex. To give the brief conclusions of Sections IV-B and IV-C, a theorem about mean and covariance of system states during forced oscillation under SCDs are presented in the following, which could be used directly.

Theorem 1: In a power system under SCDs, which is modeled as LSDEs (5), the mean and covariance of system states over time can be deduced as

$$\begin{cases} E[\Delta \boldsymbol{X}(t)] = \exp[\boldsymbol{A}(t-t_0)]\Delta \boldsymbol{X}(t_0) \\ Var[\Delta \boldsymbol{X}(t)] = \boldsymbol{P}\left\{\left[\boldsymbol{P}^{-1}\boldsymbol{K}\boldsymbol{K}^T\left(\boldsymbol{P}^{-1}\right)^T \circ \boldsymbol{J}\right]\right\}P^T \end{cases} \tag{26}$$

where exp[$\boldsymbol{A}(t-t_0)$] denotes an exponential function of $\boldsymbol{A}(t-t_0)$, see (6); "$\circ$" denotes Hadamard product [41]; $\boldsymbol{J}$ denotes a matrix whose $(i, j)^{\text{th}}$ element is $\{\exp[(\lambda_i + \lambda_j)(t-t_0)] - 1\}/(\lambda_i + \lambda_j)$; λ_i (λ_j) is the i^{th} (j^{th}) eigenvalue of $\boldsymbol{A}$, and equals to the i^{th} (j^{th}) diagonal entries of $\boldsymbol{\Lambda}$; and $\boldsymbol{P}\boldsymbol{\Lambda}\boldsymbol{P}^{-1} = \boldsymbol{A}$.

D. Stationary Distribution of System States During Forced Oscillation Under SCDs

In this section, the stationary distribution of system states during the forced oscillation under SCDs will be deduced.

Because the system is small-signal stable, all the eigenvalues (i.e., $\lambda_1, \lambda_2, \ldots, \lambda_i, \ldots$) of system state matrix $\boldsymbol{A}$ have negative real parts. Thus, one obtains

$$\lim_{t\to+\infty} \exp(\lambda_i t) = 0 \tag{27}$$

and then

$$\lim_{t\to+\infty} \exp(\boldsymbol{A}t) = \boldsymbol{O}. \tag{28}$$

By employing (28), the limit of system states mean in (26) can be deduced as

$$\lim_{t\to+\infty} E[\Delta \boldsymbol{X}(t)] = \lim_{t\to+\infty} \exp[\boldsymbol{A}(t-t_0)]\Delta \boldsymbol{X}(t_0) = \boldsymbol{O}. \tag{29}$$

By using (27), the following formulation can be obtained.

$$\begin{aligned} \lim_{t\to+\infty} \boldsymbol{J}(i,j) &= \lim_{t\to\infty}\left\{\exp\left[\left(\lambda_i + \lambda_j\right)(t-t_0)\right] - 1\right\}/\left(\lambda_i + \lambda_j\right) \\ &= \left\{\lim_{t\to\infty}\exp\left[\left(\lambda_i + \lambda_j\right)(t-t_0)\right] - 1\right\}/\left(\lambda_i + \lambda_j\right) \\ &= -1/\left(\lambda_i + \lambda_j\right) = \boldsymbol{T}(i,j) \end{aligned} \tag{30}$$

where $\boldsymbol{J}(i,j)$ denotes the $(i,j)^{\text{th}}$ element of $\boldsymbol{J}$; and $\boldsymbol{T}$ denotes a matrix whose $(i,j)^{\text{th}}$ element $\boldsymbol{T}(i,j)$ is $-1/(\lambda_i + \lambda_j)$, which is finite due to the denominator's negative real part.

Substituting (30) into $Var[\Delta \boldsymbol{X}(t)]$ in (26), one can obtain the limit of system states covariance matrix as follows:

$$\begin{aligned} \lim_{t\to+\infty} Var[\Delta \boldsymbol{X}(t)] &= \boldsymbol{P}\left\{\left[\boldsymbol{P}^{-1}\boldsymbol{K}\boldsymbol{K}^T\left(\boldsymbol{P}^{-1}\right)^T \circ \lim_{t\to\infty}\boldsymbol{J}\right]\right\}P^T \\ &= \boldsymbol{P}\left\{\left[\boldsymbol{P}^{-1}\boldsymbol{K}\boldsymbol{K}^T\left(\boldsymbol{P}^{-1}\right)^T\right] \circ \boldsymbol{T}\right\}\boldsymbol{P}^T. \end{aligned} \tag{31}$$

It can be seen that both the mean and covariance of system states have a convergence, which can be calculated by (29) and (31), respectively. By (31), the i^{th} diagonal element in the $\lim_{t\to+\infty} Var[\Delta \boldsymbol{X}(t)]$ represents the stationary variance of i^{th} system state x_i in $\Delta \boldsymbol{X}(t)$; and the stationary mean of all system states equals to zero by (29). Based on that all system states of LSDEs follow Gaussian distributions [39], the stationary probability density function of i^{th} system state x_i is deduced as follows:

$$f(x_i) = \exp\left[-x_i^2/\sigma^2\right]/\left(2\pi\sigma^2\right)^{0.5} \tag{32}$$

where σ^2 denotes the variance of i^{th} system state x_i and equals to the i^{th} diagonal element of $\lim_{t\to+\infty} Var[\Delta \boldsymbol{X}(t)]$ (31).

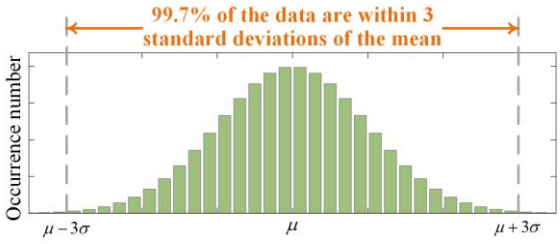

Fig. 2. Three-sigma rule for the Gaussian distribution.

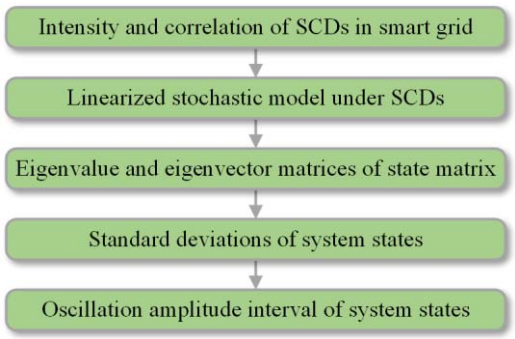

Fig. 3. The procedure of the analytic method for forced oscillation amplitude estimation in the power system under SCDs.

E. Amplitude Estimation of System States During Forced Oscillation Under SCDs

Based on the three-sigma rule, "nearly all" values following a Gaussian distribution are taken to lie within three standard deviations, i.e., that it is useful to treat 99.7% probability as "near certainty" [42]. In other words, "nearly all" system states of LSDEs (5) fall within the corresponding three-sigma interval $[-3\sigma,\ 3\sigma]$, as shown in Fig. 2. Employing the stationary variance of the system states in (31), one can easily estimate the amplitude of system states during the forced oscillation under SCDs.

The procedure of the amplitude estimation scheme is outlined below and shown in Fig. 3.

Step 1: Obtain the intensity and correlation of SCDs in power systems by statistical data.

Step 2: Build the stochastic linearized model of the system under SCDs (5).

Step 3: Solve for the eigenvalue and eigenvector matrices of system state matrix $\boldsymbol{A}$.

Step 4: Calculate stationary covariance matrix (31) by (26), and then get the standard deviations of system states.

Step 5: Estimate the amplitudes of system states during the forced oscillation under SCDs, based on the three-sigma rule.

V. Case Study

A. Monte Carlo Simulation

In this paper, Monte Carlo simulation is adopted to verify the accuracy and efficiency of the stochastic analytic method.

In Monte Carlo simulation, the simulation methods for solving LSDEs are necessary. There are several simulation methods for solving LSDEs (5), such as the Euler–Maruyama, Milstein, Runge–Kutta, and Heun's methods. In this paper,

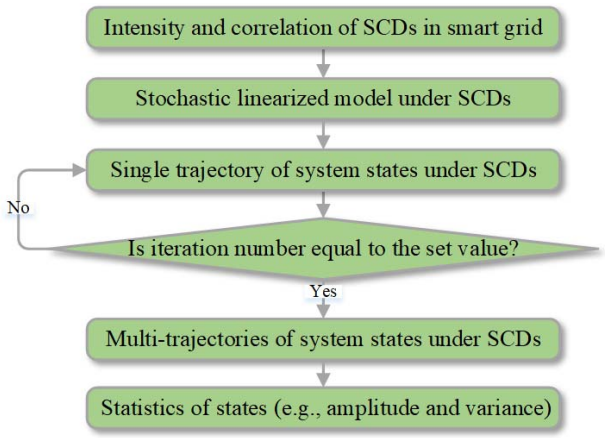

Fig. 4. The procedure of Monte Carlo simulation in this paper.

Heun's method is used, which is a predictor-corrector method. Based on Heun' method [43], one calculates the intermediate value $\Delta\hat{\boldsymbol{X}}(t_i)$ and then the final approximation at the next integration point $\Delta\boldsymbol{X}(t_{i+1})$, which is as follows:

$$\begin{cases} \Delta\boldsymbol{X}(t_{i+1}) = \Delta\boldsymbol{X}(t_i) + \boldsymbol{A}\left[\Delta\boldsymbol{X}(t_i) + \Delta\hat{\boldsymbol{X}}(t_i)\right]\frac{\Delta t}{2} \\ \qquad\qquad + \boldsymbol{K}[\boldsymbol{B}(t_{i+1}) - \boldsymbol{B}(t_i)] \\ \Delta\hat{\boldsymbol{X}}(t_i) = \Delta\boldsymbol{X}(t_i) + \boldsymbol{A}\Delta\boldsymbol{X}(t_i)\Delta t + \boldsymbol{K}[\boldsymbol{B}(t_{i+1}) - \boldsymbol{B}(t_i)] \end{cases}$$

where Δt denotes the time step of the simulation and $t_{i+1} - t_i = \Delta t$; and $\boldsymbol{B}(t_{i+1}) - \boldsymbol{B}(t_i)$ denotes the increment vector of Wiener's process.

In this study, Monte Carlo simulation means the repeated simulation of (5) and statistical analysis. The procedure of Monte Carlo simulation is outlined below and shown in Fig. 4.

Step 1: Obtain the intensity and correlation of SCDs in power systems by the statistical data.

Step 2: Build the stochastic linearized model of the system under SCDs. In this paper, the stochastic linearized model is expressed in the matrix form (5).

Step 3: Simulate a single trajectory of system states by the stochastic model. In the Monte Carlo simulation, the single trajectory is not enough, so the repeated simulations are needed. This step can be regarded as one trial of the Monte Carlo simulation.

Step 4: Execute Step 3, if the iteration number is not equal to the set value; go to Step 5, if the iteration number is equal to the set value. After the repeated simulations, the multi-trajectories of system states under SCDs can be obtained.

Step 5: Calculate the statistics of the system states. In this paper, the amplitude, mean and variance are mainly considered.

B. SMIB Power System

A modified SMIB power system in [10] is employed as the first simulation system. In this system, a wind farm connects with the infinite bus, as shown in Fig. 5. The wind farm is equivalent to an asynchronous wind turbine generator.

The SCDs are considered as the stochastic mechanical power inputs of the wind turbine generator. Then, the stochastic model of this power system can be expressed as LSDEs (5).

Fig. 5. One wind farm connecting with the infinite bus system.

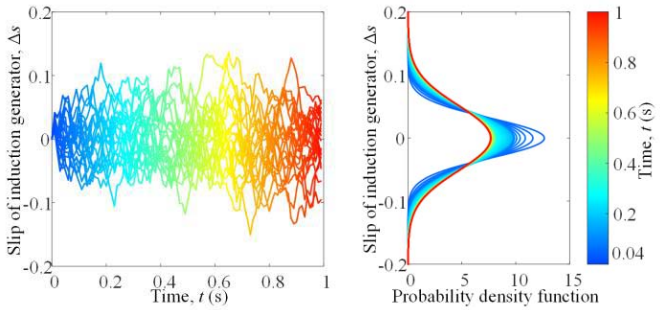

Fig. 6. The slip of the induction generator Δs during the forced oscillation. (a) 20 trajectories. (b) Probability density function.

There are three system states in this system, the real part of transient potential ΔE_r', the imaginary part of transient potential ΔE_m', and the slip of the induction generator Δs. Based on the parameters given in [10], both the system state matrix $\boldsymbol{A}$ and the covariance matrix of SCDs $\boldsymbol{K}$ for (5) are shown as follows:

$$\boldsymbol{A} = \begin{bmatrix} -6.1678 & -2.2854 & -78.1942 \\ 2.2854 & -6.1678 & -267.69 \\ 0.0105 & 0.6632 & 0 \end{bmatrix}$$
$$\text{and } \boldsymbol{K} = \begin{bmatrix} 0 & 0 & 0 \\ 0 & 0 & 0 \\ 0 & 0 & 0.1642 \end{bmatrix} \tag{33}$$

where there is one nonzero element in the covariance matrix $\boldsymbol{K}$, because the SCDs describing the stochastic mechanical power inputs are added to the electromechanical equation.

The Heun' method is used to obtain trajectories of system states under SCDs. Fig. 6 (a) shows 20 trajectories of the slip of the induction generator Δs during the forced oscillation under SCDs, from which it is difficult to find the statistics directly. To illustrate the stochastic characteristics of system states during forced oscillation, Fig. 6 (b) shows the probability density function of Δs during the forced oscillation. It can be seen that the probability density function of Δs converges to a certain distribution over time, which means the system state Δs has a stationary distribution. In other words, the oscillation behavior of a power system under SCDs is randomly "steady-state" after a certain time. By the stochastic analysis in Section IV-C, the stationary distribution is theoretically explained and its probability density function analytically calculated by (32) directly.

The stationary distributions clearly reflect the characteristics of the forced oscillation under SCDs. Because the stationary distribution of a system state is a Gaussian distribution, the stationary variance and mean are of great interest to study. For the SMIB power system, the stationary variances and means of system states are calculated by Monte Carlo simulation and the proposed method, which are shown in Table I. Clearly, the results of the analytic method are very close to Monte Carlo simulation results, which demonstrate that the proposed method is similarly accurate comparing with Monte Carlo simulation.

TABLE I
COMPARISONS OF STATIONARY VARIANCE AND MEAN FROM MONTE CARLO SIMULATION AND THE PROPOSED METHOD

State variables	Stationary variances		Stationary mean	
	Monte Carlo simulation	the proposed method	Monte Carlo simulation	the proposed method
ΔE_r'	5.4997×10^{-2}	5.5681×10^{-2}	2.2947×10^{-3}	0
ΔE_m'	9.1528×10^{-1}	9.3670×10^{-1}	8.8297×10^{-3}	0
Δs	2.6908×10^{-3}	2.7137×10^{-3}	-6.4913×10^{-4}	0

TABLE II
EIGENVALUE ANALYSIS REPORT OF THE MODIFIED IEEE 14-BUS CASE

Name	Number
Dynamic order	48
Buses	14
Eigenvalues with positive real parts	0
Eigenvalues with negative real parts	48
Complex pairs of eigenvalues	9
Zero eigenvalues	0

Furthermore, the stationary standard deviation values of system states ΔE_r', ΔE_m', and Δs are calculated as 0.2360, 0.9678, and 0.0521, respectively. Based on the proposed amplitude estimation scheme, the amplitudes of ΔE_r', ΔE_m', and Δs are estimated as 0.7079, 2.9035, and 0.1563, respectively. In Figs. 7 (a)-(c), 20 trajectories and the corresponding estimated amplitudes of the three system states are shown by solid and dotted lines, respectively. It can be seen that most parts of trajectories are within the corresponding estimated amplitudes, which verifies the effectiveness of the proposed scheme.

C. Modified IEEE 14-Bus Case Study

To demonstrate the scalability of the proposed stochastic analytic method on multi-machine power systems under SCDs, a modified IEEE 14-bus case is adopted as shown in Fig. 8.

This modified case is included in MATLAB-based Power System Analysis Toolbox (PSAT) [44]. From PSAT, one also can find the detailed description of dynamic and static parameters for this case. In this modified IEEE 14-bus case, there is a wind farm (i.e., G1-DFIG) connecting to Bus 1, which is equivalent as a doubly fed induction generator with a variable speed wind turbine in PSAT. Also, there are four synchronous machines (i.e., G2, G3, G4, and G5) connecting to Bus 2, Bus 3, Bus 8, and Bus 6, which are modeled by fourth-order synchronous machine models. All loads are described by the constant impedance models. A simple eigenvalue analysis report from PSAT is given in Table II. It can be seen that there are 48 system states and all eigenvalues have negative real parts in this modified IEEE 14-bus case.

The renewable energy generation from G1-DFIG is 90.8% of the total generation in the system, which means the system

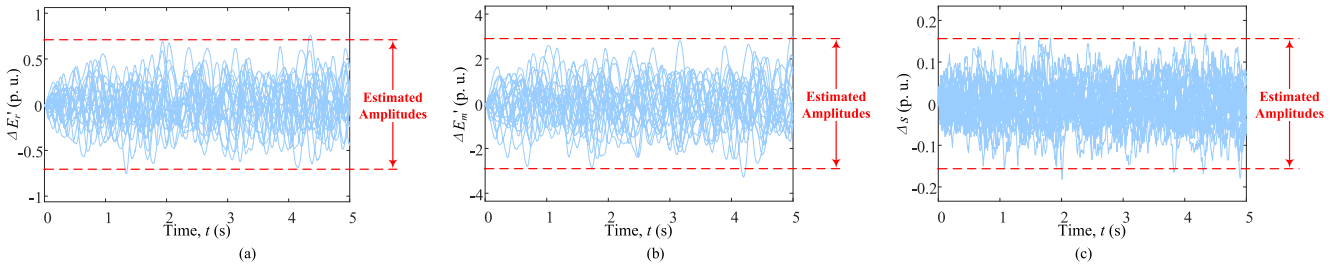

Fig. 7. Amplitude estimation of system states under SCDs. (a) ΔE_r'. (b) ΔE_m'. (c) Δs.

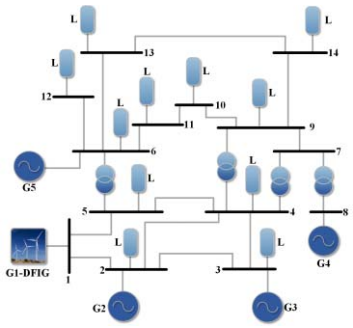

Fig. 8. A modified IEEE 14-bus case.

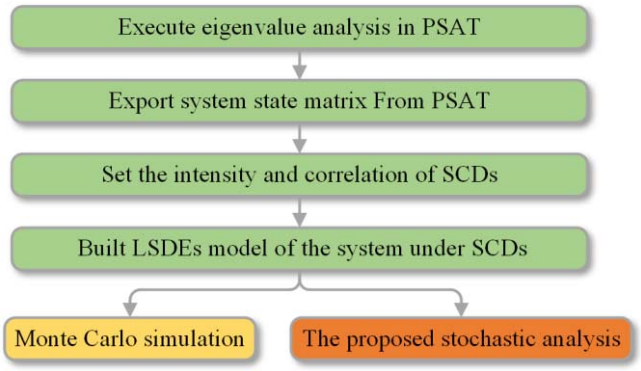

Fig. 9. The procedure of Monte Carlo simulation and the proposed stochastic analysis in a modified IEEE 14-bus case.

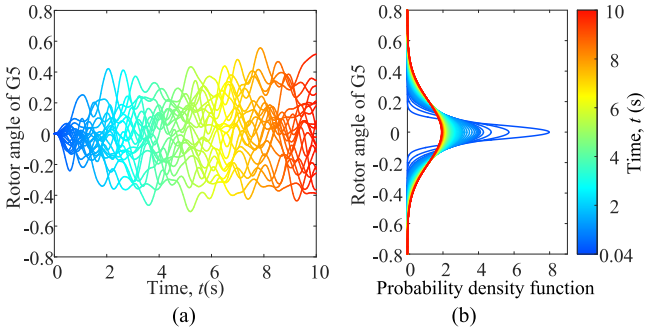

Fig. 10. The rotor angle of the generator G5 during the forced oscillation. (a) 20 trajectories. (b) Probability density function.

is highly penetrated by renewable energy. With the high penetration renewable energy in this system, the SCDs becomes considerable. The SCDs are assumed from the mechanical power input of wind turbine G1-DFIG, due to the stochastic nature of wind. Then the electromechanical equation of wind generator can be expressed as [10], [30], and [35]–[37]

$$2H_m \mathrm{d}\omega = (P_m - P_e)\mathrm{d}t + \sigma \mathrm{d}B(t) \tag{34}$$

where H_m denotes rotor inertia; ω denotes angular frequency; P_m denotes mechanical power; P_e denotes electrical power; $\sigma \mathrm{d}B(t)$ denotes the SCDs; $B(t)$ denotes a standard Wiener process; and σ denotes the intensity of SCDs. In this case, the intensity of the SCDs σ is set as $0.0333Pm$.

After the consideration of SCDs, the system can be described by a set of SDAEs (3). However, no mature commercial software could simulate SDAEs directly. In this paper, to implement the stochastic analysis of forced oscillation, PSAT is initially used to obtain the system state matrix $\boldsymbol{A}$, and then a separate MATLAB program is coded to simulate the LSDEs (5). PSAT is a user-friendly open-source MATLAB software program. One can export the system state matrix $\boldsymbol{A}$ from PSAT after the eigenvalue analysis is executed. Based on the exported system state matrix $\boldsymbol{A}$, the LSDEs model (5) for this modified IEEE 14-bus case is built. Furthermore, the analysis of the forced oscillation under SCDs can be carried on with the LSDEs (5). To promote repeatability of the simulation, a flowchart is given to illustrate the simulation process of Monte Carlo simulation and the proposed stochastic analysis, which is shown in Fig. 9.

By using the Heun' method, 20 rotor angle trajectories of G5 are shown in Fig. 10 (a). Furthermore, the probability density function of rotor angle of G5 over time is shown in Fig. 10 (b), from which the phenomenon that the rotor angle has a stationary distribution is found. Actually, the same phenomenon is found for all the system states in this case, but only the rotor angle of G5 is illustrated here.

Let ω_1, ω_2, ω_3, ω_4, and ω_5 denote the rotor speed deviations of the five generators G1-DFIG, G2, G3, G4, and G5, respectively. By using Monte Carlo simulation and the proposed analytic method, the variances of ω_1, ω_2, ω_3, ω_4, and ω_5 are calculated, as shown in Table III. It can be seen that the variances from Monte Carlo simulation get closer to the stationary variances from the proposed method, when the simulation time increases, time step decreases, and iteration increases.

The computation efficiency is also important in engineering application. For this modified IEEE 14-bus case with 48 system states, it takes 0.004s to calculate stationary variances by using the proposed method. However, it takes 301.009s by Monte Carlo simulation with iteration 5000,

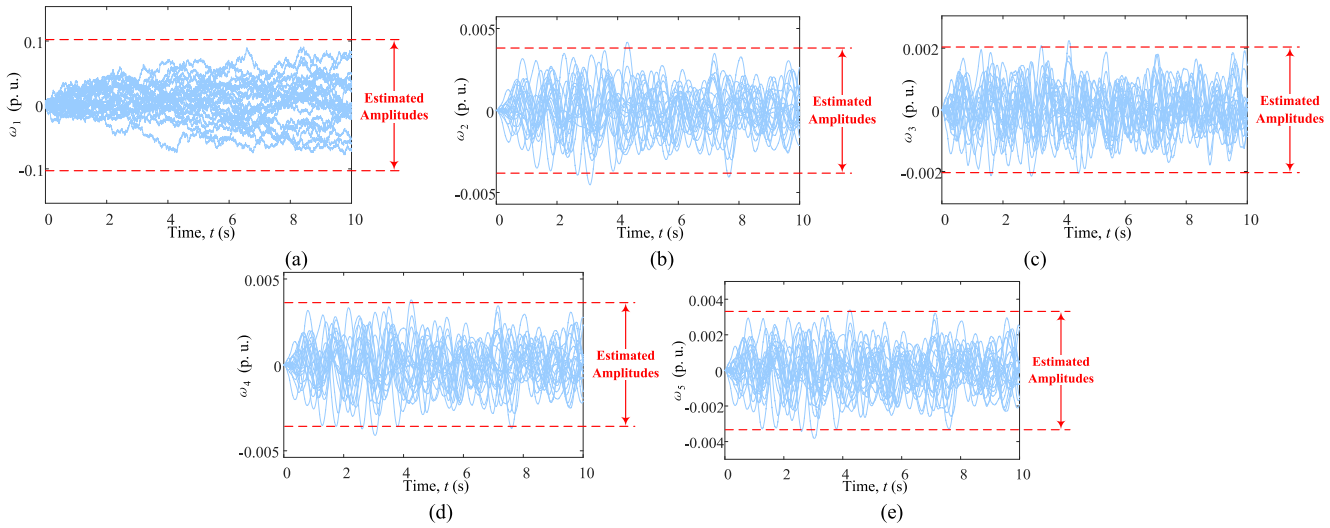

Fig. 11. Amplitude estimation of system states under SCDs. (a) ω_1. (b) ω_2. (c) ω_3. (d) ω_4. (e) ω_5.

TABLE III
COMPARISON OF VARIANCES FROM MONTE CARLO SIMULATION AND THE PROPOSED METHOD

State variables	Variances from Monte Carlo simulation			Stationary variances from the proposed method
	iteration 2500, simulation time 5s, time step 0.002s,	iteration 5000, simulation time 10s, time step 0.001s	iteration 10000, simulation time 20s, time step 0.0005s	
ω_1	8.1500×10^{-4}	1.1005×10^{-3}	1.1588×10^{-3}	1.1706×10^{-3}
ω_2	1.5248×10^{-6}	1.5865×10^{-6}	1.6223×10^{-6}	1.6158×10^{-6}
ω_3	4.5546×10^{-7}	4.5645×10^{-7}	4.5752×10^{-7}	4.5917×10^{-7}
ω_4	1.3697×10^{-6}	1.4018×10^{-6}	1.4469×10^{-6}	1.4342×10^{-6}
ω_5	1.1870×10^{-6}	1.2108×10^{-6}	1.2436×10^{-6}	1.2354×10^{-6}

simulation time 10s, and time step 0.001s, and the result accuracy by this Monte Carlo simulation is not very high, see Table III. From the aspect of efficiency, the proposed analytic method is many orders of magnitude faster than Monte Carlo simulation.

With the calculated stationary variances of ω_1, ω_2, ω_3, ω_4, and ω_5, one can easily estimate the amplitudes of those system states as 0.1026, 0.0038, 0.0020, 0.0036 and 0.0033, respectively, by using the proposed amplitude estimation scheme shown in Fig. 3. In Figs. 11 (a)-(e), 20 trajectories and the corresponding estimated amplitudes of the five system states are shown by solid and dotted lines, respectively. Clearly, most parts of system states' trajectories are within the corresponding estimated amplitudes, which verifies the effectiveness of the proposed scheme in a multi-machine power system under SCDs.

VI. CONCLUSION

With the challenges of randomness from the intermittent renewable energy, an efficient analytic method for the forced oscillation under SCDs is desired. This paper proposes an efficient analytic method for forced oscillation under SCDs. The main contributions of this paper are as follows:

(1) A stochastic analytic method is proposed to investigate system states' statistics during forced oscillation under SCDs, which has high accuracy and offers clear impact mechanism;

(2) A novel oscillation phenomenon of power systems under SCDs, which presents system states oscillate with stationary distributions, is clearly characterized and theoretically explained;

(3) An amplitude estimation scheme is put forward to estimate oscillation amplitudes of system states under SCDs, which could be used for quickly analyzing the impacts of SCDs on the forced oscillation.

The proposed method can be used to analyze forced oscillation issues in the power system under SCDs. The proposed method has several advantages including the high efficiency and clear mechanism, which meet the needs of the power system being smarter and more intelligent. Meanwhile, the proposed method offers more scientific indexes for judging the performance of a control method under SCDs, which can be helpful to address the issues under SCDs. Facing the increasing penetrations of renewable energy and electric vehicles, we believe that the proposed method could serve well for the power system.

APPENDIX

In this Appendix, an example is given to show the power system models under SCDs. In this stochastic model, the generators are modeled by the classical model, and the loads are modeled by constant impedance models. The stochastic model of multi-machine power systems under SCDs can be expressed as a set of Itô SDEs [30], [36], [37]

$$\begin{cases} \mathrm{d}\delta_i = \omega_N \omega_i \mathrm{d}t \\ \mathrm{d}\omega_i = \frac{1}{M_i}\Big[P_{mi} - G_{ii}E_i^2 - \sum_{j=1,j\neq i}^{n} E_i E_j B_{ij}\sin\big(\delta_i - \delta_j\big) \\ \qquad\qquad - D_i\omega_i\Big]\mathrm{d}t + \frac{\sigma_i}{M_i}\mathrm{d}B_i(t) \\ \qquad i = 1, 2, \ldots, n \end{cases} \tag{A-1}$$

where $\frac{\sigma_i}{M_i}\mathrm{d}B_i(t)$ denotes SCDs; $B_i(t)$ denotes the standard Wiener processes; σ_i are disturbance intensities; δ_i, ω_i, M_i, P_{mi}, E_i and D_i are rotor angle, rotor speed deviation, inertia coefficient, mechanical power, internal voltage and damping coefficient of i^{th} generator, respectively; G_{ii} is the i^{th} diagonal

element of conductance matrix; B_{ij} is the element in the i^{th} row and j^{th} column of susceptance matrix; and ω_N is the synchronous machine speed.

Furthermore, the linearized stochastic model around the equilibrium point (i.e., the steady state) can be expressed as

$$\begin{cases} \mathrm{d}\Delta\delta_i = \omega_N \Delta\omega_i \mathrm{d}t \\ \mathrm{d}\Delta\omega_i = \frac{1}{M_i}\Big[P_{mi} - G_{ii}E_i^2 - \sum_{j=1,j\neq i}^{n} E_i E_j B_{ij}\cos\big(\delta_{is} - \delta_{js}\big) \\ \qquad\qquad \times \ \big(\Delta\delta_i - \Delta\delta_j\big) - D_i\Delta\omega_i\Big]\mathrm{d}t + \frac{\sigma_i}{M_i}\mathrm{d}B_i(t) \\ \qquad i = 1, 2, \ldots, n \end{cases} \tag{A-2}$$

where $\Delta\omega_i = \omega_i$; $\Delta\delta_i = \delta_i - \delta_n$ and $\Delta\delta_n = 0$; δ_n is the rotor angle of the n^{th} generator, which is set as the reference node.

Because there are no algebraic equations in (A-2), the linearized stochastic model can be expressed in the matrix form (5) directly.

ACKNOWLEDGMENT

The authors would like to thank the anonymous editors and reviewers for many helpful corrections and suggestions to improve the readability of this paper. The authors also gratefully acknowledge Dr. Weiqiu Zhu and Dr. Robert Mee for their guidance on this research.

REFERENCES

[1] F. Li *et al.*, "Smart transmission grid: Vision and framework," *IEEE Trans. Smart Grid*, vol. 1, no. 2, pp. 168–177, Sep. 2010.

[2] W. Su, J. Wang, and J. Roh, "Stochastic energy scheduling in microgrids with intermittent renewable energy resources," *IEEE Trans. Smart Grid*, vol. 5, no. 4, pp. 1876–1883, Jul. 2014.

[3] Q. Xu *et al.*, "A probabilistic method for determining grid-accommodable wind power capacity based on multiscenario system operation simulation," *IEEE Trans. Smart Grid*, vol. 7, no. 1, pp. 400–409, Jan. 2016.

[4] H. Li *et al.*, "Stochastic stability analysis of the power system with losses," *Energies*, vol. 11, no. 3, p. 678, 2018.

[5] D. Molina, G. K. Venayagamoorthy, J. Liang, and R. G. Harley, "Intelligent local area signals based damping of power system oscillations using virtual generators and approximate dynamic programming," *IEEE Trans. Smart Grid*, vol. 4, no. 1, pp. 498–508, Mar. 2013.

[6] R. Preece and J. Milanović, "Efficient estimation of the probability of small-disturbance instability of large uncertain power systems," *IEEE Trans. Power Syst.*, vol. 31, no. 2, pp. 1063–1072, Mar. 2016.

[7] Y. Pan *et al.*, "Admissible region of large-scale uncertain wind generation considering small-signal stability of power systems," *IEEE Trans. Sustain. Energy*, vol. 7, no. 4, pp. 1611–1623, Oct. 2016.

[8] K. N. Hasan, R. Preece, and J. V. Milanović, "Priority ranking of critical uncertainties affecting small-disturbance stability using sensitivity analysis techniques," *IEEE Trans. Power Syst.*, vol. 32, no. 4, pp. 2629–2639, Jul. 2017.

[9] S. Eftekharnejad, V. Vittal, G. T. Heydt, B. Keel, and J. Loehr, "Small signal stability assessment of power systems with increased penetration of photovoltaic generation: A case study," *IEEE Trans. Sustain. Energy*, vol. 4, no. 4, pp. 960–967, Oct. 2013.

[10] B. Yuan, M. Zhou, G. Li, and X.-P. Zhang, "Stochastic small-signal stability of power systems with wind power generation," *IEEE Trans. Power Syst.*, vol. 30, no. 4, pp. 1680–1689, Jul. 2015.

[11] J. Zhang, P. Ju, Y. Yu, and F. Wu, "Responses and stability of power system under small Gauss type random excitation," *Sci. China Technol. Sci.*, vol. 55, no. 7, pp. 1873–1880, Jul. 2012.

[12] R. Billinton and W. Li, *Reliability Assessment of Electric Power Systems Using Monte Carlo Methods*, 1st ed. New York, NY, USA: Plenum, 1994.

[13] Z. Xu, M. Ali, Z. Y. Dong, and X. Li, "A novel grid computing approach for probabilistic small signal analysis," in *Proc. IEEE Power Eng. Soc. Gen. Meeting*, Montreal, QC, Canada, 2006, p. 8, doi: 10.1109/PES.2006.1709449.

[14] J. L. Rueda, D. G. Colome, and I. Erlich, "Assessment and enhancement of small signal stability considering uncertainties," *IEEE Trans. Power Syst.*, vol. 24, no. 1, pp. 198–207, Feb. 2009.

[15] S. Q. Bu *et al.*, "Probabilistic analysis of small-signal stability of large-scale power systems as affected by penetration of wind generation," *IEEE Trans. Power Syst.*, vol. 27, no. 2, pp. 762–770, May 2012.

[16] X. Y. Bian, Y. Geng, K. L. Lo, Y. Fu, and Q. B. Zhou, "Coordination of PSSs and SVC damping controller to improve probabilistic small-signal stability of power system with wind farm integration," *IEEE Trans. Power Syst.*, vol. 31, no. 3, pp. 2371–2382, May 2016.

[17] S. Q. Bu, W. Du, and H. F. Wang, "Investigation on probabilistic small-signal stability of power systems as affected by offshore wind generation," *IEEE Trans. Power Syst.*, vol. 30, no. 5, pp. 2479–2486, Sep. 2015.

[18] H. Huang, C. Y. Chung, K. W. Chan, and H. Chen, "Quasi-Monte Carlo based probabilistic small signal stability analysis for power systems with plug-in electric vehicle and wind power integration," *IEEE Trans. Power Syst.*, vol. 28, no. 3, pp. 3335–3343, Aug. 2013.

[19] Y. Zhou *et al.*, "The stochastic response surface method for small-signal stability study of power system with probabilistic uncertainties in correlated photovoltaic and loads," *IEEE Trans. Power Syst.*, vol. 32, no. 6, pp. 4551–4559, Nov. 2017.

[20] S. Liu, P. X. Liu, and X. Wang, "Stochastic small-signal stability analysis of grid-connected photovoltaic systems," *IEEE Trans. Ind. Electron.*, vol. 63, no. 2, pp. 1027–1038, Feb. 2016.

[21] J. Qui, S. M. Shahidehpour, and Z. Schuss, "Effect of small random perturbations on power systems dynamics and its reliability evaluation," *IEEE Trans. Power Syst.*, vol. 4, no. 1, pp. 197–204, Feb. 1989.

[22] J. Qui, S. M. Shahidehpour, and Z. Schuss, "Random perturbation of transfer capability and its effect on power system reliability evaluation," *Int. J. Elect. Power Energy Syst.*, vol. 11, no. 4, pp. 253–266, Oct. 1989.

[23] K. Loparo and G. Blankenship, "A probabilistic mechanism for small disturbance instabilities in electric power systems," *IEEE Trans. Circuits Syst.*, vol. 32, no. 2, pp. 177–184, Feb. 1985.

[24] S. V. Dhople, Y. C. Chen, L. DeVille, and A. D. Dominguez-Garcia, "Analysis of power system dynamics subject to stochastic power injections," *IEEE Trans. Circuits Syst. I, Reg. Papers*, vol. 60, no. 12, pp. 3341–3353, Dec. 2013.

[25] G. Ghanavati, P. D. H. Hines, and T. I. Lakoba, "Identifying useful statistical indicators of proximity to instability in stochastic power systems," *IEEE Trans. Power Syst.*, vol. 31, no. 2, pp. 1360–1368, Mar. 2016.

[26] Y. C. Chen and A. D. Dominguez-Garcia, "A method to study the effect of renewable resource variability on power system dynamics," *IEEE Trans. Power Syst.*, vol. 27, no. 4, pp. 1978–1989, Nov. 2012.

[27] H. Mohammed and C. O. Nwankpa, "Stochastic analysis and simulation of grid-connected wind energy conversion system," *IEEE Trans. Energy Convers.*, vol. 15, no. 1, pp. 85–90, Mar. 2000.

[28] T. Odun-Ayo and M. L. Crow, "Structure-preserved power system transient stability using stochastic energy functions," *IEEE Trans. Power Syst.*, vol. 27, no. 3, pp. 1450–1458, Aug. 2012.

[29] Z. Y. Dong, J. H. Zhao, and D. J. Hill, "Numerical simulation for stochastic transient stability assessment," *IEEE Trans. Power Syst.*, vol. 27, no. 4, pp. 1741–1749, Nov. 2012.

[30] K. Wang and M. L. Crow, "The Fokker–Planck equation for power system stability probability density function evolution," *IEEE Trans. Power Syst.*, vol. 28, no. 3, pp. 2994–3001, Aug. 2013.

[31] F. Milano and R. Zárate-Miñano, "A systematic method to model power systems as stochastic differential algebraic equations," *IEEE Trans. Power Syst.*, vol. 28, no. 4, pp. 4537–4544, Nov. 2013.

[32] X. Wang, H.-D. Chiang, J. Wang, H. Liu, and T. Wang, "Long-term stability analysis of power systems with wind power based on stochastic differential equations: Model development and foundations," *IEEE Trans. Sustain. Energy*, vol. 6, no. 4, pp. 1534–1542, Oct. 2015.

[33] R. Zárate-Miñano, M. Anghel, and F. Milano, "Continuous wind speed models based on stochastic differential equations," *Appl. Energy*, vol. 104, pp. 42–49, Apr. 2013.

[34] H. Ye, Y. Liu, P. Zhang, and Z. Du, "Analysis and detection of forced oscillation in power system," *IEEE Trans. Power Syst.*, vol. 32, no. 2, pp. 1149–1160, Mar. 2017.

[35] J. C. Pidre, C. J. Carrillo, and A. E. F. Lorenzo, "Probabilistic model for mechanical power fluctuations in asynchronous wind parks," *IEEE Trans. Power Syst.*, vol. 18, no. 2, pp. 761–768, May 2003.

[36] P. Ju *et al.*, "Stochastic dynamic analysis for power systems under uncertain variability," *IEEE Trans. Power Syst.*, vol. 33, no. 4, pp. 3789–3799, Jul. 2018, doi: 10.1109/TPWRS.2017.2777783.

[37] P. Ju *et al.*, "Analytical assessment for transient stability under stochastic continuous disturbances," *IEEE Trans. Power Syst.*, vol. 33, no. 2, pp. 2004–2014, Mar. 2018.
[38] G. Golub and C. Van Loan, *Matrix Computations*, 1st ed. Baltimore, MD, USA: Johns Hopkins Univ. Press, 1996.
[39] X. Mao, *Stochastic Differential Equations and Their Applications*, 1st ed. Chichester, U.K.: Horwood, 1997.
[40] M. Ghorbaniparvar, N. Zhou, X. Li, D. Trudnowski, and R. Xie, "A forecasting-residual spectrum analysis method for distinguishing forced and natural oscillations," *IEEE Trans. Smart Grid*, to be published.
[41] R. Horn and C. Johnson, *Matrix Analysis*. New York, NY, USA: Cambridge Univ. Press, 2013.
[42] F. Pukelsheim, "The three sigma rule," *Amer. Statistician*, vol. 48, no. 2, pp. 88–91, 1994.
[43] R. Bains, "Introduction to applied numerical analysis," *Eng. Anal. Boundary Elements*, vol. 10, no. 1, p. 88, 1992.
[44] F. Milano. (2017). *Federico Milano*. Accessed: May 26, 2017. [Online]. Available: http://faraday1.ucd.ie/psat.html

Hongyu Li (S'14) received the B.S. degree in electrical engineering from North China University of Water Resources and Electric Power, Zhengzhou, China, in 2012. He is currently pursuing the Ph.D. degree in electrical engineering with Hohai University, Jiangsu, China. He is currently a visiting student with the University of Tennessee, Knoxville, TN, USA.

His research interests include power system dynamic analysis under stochastic disturbances.

Ping Ju (M'95–SM'10) received the B.S. and M.S. degrees in electrical engineering from Southeast University, Nanjing, China, in 1982 and 1985, respectively, and the Ph.D. degree in electrical engineering from Zhejiang University, Hangzhou, China. From 1994 to 1995, he was an Alexander-von Humboldt Fellow with the University of Dortmund, Germany. He is currently a Professor of electrical engineering with Hohai University, Nanjing, China.

His research interest includes modeling and control of power system.

Chun Gan (S'14–M'16) received the Ph.D. degree in electrical engineering from Zhejiang University, Hangzhou, China, in 2016.

He is currently a Research Associate with the Department of Electrical Engineering and Computer Science, University of Tennessee, Knoxville, TN, USA. He was a recipient of the 2018 Marie Sklodowska-Curie Actions Seal of Excellence from European Commission, the 2015 Top Ten Excellent Scholar Award, the 2016 Excellent Ph.D. Graduate Award, the 2015 Ph.D. National Scholarship, the 2015 Wang Guosong Scholarship, and the 2014 and 2015 Outstanding Ph.D. Candidate Awards in Zhejiang University.

Dr. Gan's research interests include high-efficiency power converters, electric vehicles, electrical motor drives, continuous variable series reactors, high-voltage direct current transmission, and microgrids.

Yufei Tang (M'16) received the B.Eng. and M.Eng. degrees from Hohai University, Nanjing, China, in 2008 and 2011, respectively, and the Ph.D. degree in electrical engineering from ECBE Department, University of Rhode Island, Kingston, RI, USA, in 2016. He is currently an Assistant Professor with CEECS Department, and a Faculty Fellow with I-SENSE, Florida Atlantic University, Boca Raton, FL, USA.

His research interests include machine learning, data mining, cyber-physical systems, and smart grid.

Yiping Yu (M'10) received the B.Sc. and M.Sc. degrees in electrical engineering from Sichuan University, Chengdu, China, in 1999 and 2002, respectively, and the Ph.D. degree in electrical engineering from Tsinghua University, Beijing, China, in 2010. He is an Associate Professor with the College of Energy and Electrical Engineering, Hohai University, Nanjing, China. From 2013 to 2014, he was also a Visiting Scholar with the Georgia Institute of Technology, GA, USA. From 2002 to 2006, he was an EMS Engineer with China Electric Power Research Institute, Beijing.

His research interest includes power system stability and control.

Yilu Liu (S'88–M'89–SM'99–F'04) received the B.S. degree from Xi'an Jiaotong University, China, and the M.S. and Ph.D. degrees from Ohio State University, Columbus, OH, USA, in 1986 and 1989, respectively. From 2001 to 2009, she was a Professor with Virginia Tech, VA, USA. She is currently the Governor's Chair with the University of Tennessee, Knoxville, TN, USA, and Oak Ridge National Laboratory (ORNL), Oak Ridge, TN, USA. She is elected as a member of the National Academy of Engineering in 2016. She is also the Deputy Director of the DOE/NSF co-funded engineering research center CURENT. She led the effort to create the North American power grid Frequency Monitoring Network with Virginia Tech, which is currently operated with UTK and ORNL as GridEye.

Her current research interests include power system wide-area monitoring and control, large interconnection-level dynamic simulations, electromagnetic transient analysis, and power transformer modeling and diagnosis.